

Supplementary information

Understanding high-salt and cold adaptation of a polyextremophilic enzyme

Ram Karan^{1*}, Sam Mathew¹, Reyhan Muhammad², Didier B. Bautista¹, Malvina Vogler¹, Romina Oliva^{1,3}, Luigi Cavallo¹, Stefan T. Arold^{2,4*}, Magnus Rueping^{1*}

¹King Abdullah University of Science and Technology (KAUST), KAUST Catalysis Center, Thuwal 23955-6900, Saudi Arabia

²King Abdullah University of Science and Technology (KAUST), Computational Bioscience Research Center (CBRC), Biological and Environmental Science and Engineering (BESE), Thuwal, 23955-6900, Saudi Arabia

³Department of Sciences and Technologies, University Parthenope of Naples, Centro Direzionale Isola C4, I-80143 Naples, Italy

⁴Centre de Biochimie Structurale, CNRS, INSERM, Université de Montpellier, 34090 Montpellier, France

*Corresponding author: Ram Karan, ram.karan@kaust.edu.sa, Stefan T. Arold, stefan.arold@kaust.edu.sa; Magnus Rueping, magnus.rueping@kaust.edu.sa

Index:

Table S1. Oligonucleotides used in this study

Table S2: Biochemical properties of crystalized β -galactosidases from GH42 family.

Table S3. β -galactosidase sequence identity matrix (Family 42)

Table S4. Structural homologs (DALI) of β -galactosidase from *Halorubrum lacusprofundi*

Table S5. Trends for halo-, psychro and thermoadaptation compared mesophilic proteins

Table S6. Differences in residue RMSF values (Δ RMSF) between 47 and 10 °C for eight functionally relevant residues.

Figure S1. Shuttle vector for the expression of bga in *Haloferax volcanii*

Figure S2. X-gal hydrolysis

Figure S3. Coomassie and InVision His-tag In-gel stained SDS-PAGE, tryptic digest and LC-MS/MS analysis of β -galactosidase

Figure S4. MALDI-TOF analysis of purified β -galactosidase

Figure S5. Measured melting curve and fitting curve

Figure S6. Structural assessment of hla_bga homology model produced by Swiss Modeller

30 Figure S7. Sequence alignment based on Hidden Markov Model (HMM) profiles, obtained with HHPRED
31 Figure S8. β -D-galactose binding pocket.

32 Figure S9. Ratio of amino acids in hla_bga and its structural homologs

33 Figure S10. Superimposed β -Galactosidase monomers.

34 Figure S11. Ratio of amino acids on the solvent-exposed surface in the hla_bga and its structural
35 homologs.

36 Figure S12. Backbone RMSD plots over time for the three independent simulations of the three
37 investigated systems at the four explored temperatures (10, 27, 47 and 72 °C).

38 Figure S13. Effect of temperature on the hla_bga monomer and trimer backbone RMSD.

39 Figure S14. RMSF values averaged over the last 20 ns of the three simulations ran for each investigated
40 system at 10, 27, 47 and 72 °C.

41

42 **Table S1. Oligonucleotides used in this study**

43

Primer	5'-3' sequence	Use
7His.bga F	cggcccaacggttgattgcatatgcaccaccaccaccacca ccacATGCGTCTCGGAGTCTGTTAC	Inserting <i>bga</i> gene and 6His
7His.bga R	ggtcgactctagaactagtggatcCTACGTCTGAG CGATTCTC CCACCACCATATGATGATG	
pTA693.F	GTTCGAACCGCCCTTTCC	Sequencing of <i>bga</i> gene
pTA693.R	ATGACCATGATTACGCCAAG	

44

45

46

47

48

49

50

51

52

53

54

55

56
57
58

Table 2: Biochemical properties of crystalized β -galactosidases from GH42 family.

PDB ID	Organism	Type	Temperature range, optima (°C)	pH range, optima	Salt range, optima (M)
[1]hla_bga (current work)	<i>Halorubrum lacusprofundi</i>	Polyextremophiles	4-70, 50	6.0-8.0, 6.5	0.5-4.5, 4
[2,3]1KWG	<i>Thermus thermophilus</i> A4	Thermophile	40-90, 70	5.0-9.0, 6.5	-
[4,5]5E9A	<i>Rahnella</i> sp. R3	Psychrophile	4-45, 35	5.5-8.0, 6.5	-
[6]4UZS	<i>Bifidobacterium bifidum</i> S17	Mesophile	20-55, 40	4.0-8.0, 6.0	-
[7]3TTS	<i>Bacillus circulans</i> sp. <i>alkalophilus</i>	Mesophile	10-70, 55	4.5-10, 6.5	-
[8,9]4OIF	<i>Geobacillus stearothermophilus</i>	Thermophile	30-80, 60	4.5-10, 6.0	-
[10]4UNI	<i>Bifidobacterium animalis</i> subsp. <i>lactis</i> B1-04	Mesophile	30-70, 37	4.0-10, 6.5	-
[11]5XB7	<i>Bifidobacterium</i> species	Mesophile	37	6.5	-
[12]6Y2K	<i>Marinomonas</i> ef1	Psychrophile	55	6.0	0-2.4

59
60
61
62
63
64
65
66
67
68
69
70
71
72
73
74
75

Salt range optima of β -galactosidases other than hla_bga and 6Y2K are not available.

76
77

Table S3. β -galactosidase sequence identity matrix using Clustal Omega (Family 42)

	hla_bga	1KWG	6Y2K	4UNI	4UZS	3TTS	4OIF	5E9A	5XB7	5VYM
hla_bga	100	46	41	29	29	29	29	28	26	24
1KWG	46	100	55	29	31	31	29	33	26	21
6Y2K	41	55	100	27	27	29	27	29	27	20
4UNI	29	29	27	100	62	33	30	30	24	30
4UZS	29	31	27	62	100	35	32	33	22	37
3TTS	29	31	29	33	35	100	40	46	24	27
4OIF	29	29	27	30	32	40	100	49	23	25
5E9A	28	33	29	30	33	46	49	100	24	28
5XB7	26	26	27	24	22	24	23	24	100	23
5VYM	24	21	20	30	37	27	25	28	23	100

78 *Halorubrum lacusprofundi*, hla_bga; *Bacillus circulans* sp. Alkalophilus, 3TTS; *Bifidobacterium animalis*
79 subsp. lactis BI-04, 4UNI; *Bifidobacterium bifidum* S17, 4UZS; *Bifidobacterium adolescentis*, 5VYM;
80 *Bifidobacterium* species, 5XB7; *Marinomonas* ef1, 6Y2K; *Rahnella* sp. R3, 5E9A; *Thermus thermophilus*
81 A4, 1KWG; *Geobacillus stearothermophilus*, 4OIF.

82

83 **Table S4. Structural homologs (DALI) of β -galactosidase from *Halorubrum lacusprofundi***

#	PDB ID	Organism	Type	Z-score	Rmsd (A°)	Identity (%)
1	1KWK-A	<i>Thermus thermophilus</i> A4	Thermophile	47.1	1.5	46
2	1KWG-A	<i>Thermus thermophilus</i> A4	Thermophile	46.4	1.6	46
3	6Y2K-A	<i>Marinomonas</i> EF1	Thermophile	46.4	1.5	41
4	5E9A-A	<i>Rahnella</i> sp. R3	Psychrophile	41.3	1.8	28
5	4UCF-A	<i>Bifidobacterium bifidum</i> S17	Mesophile	40.6	2.2	29
6	4UZS-A	<i>Bifidobacterium bifidum</i> S17	Mesophile	40.3	2.3	29
7	3TTS-D	<i>Bacillus circulans</i> sp. <i>alkalophilus</i>	Mesophile	40.0	1.9	29
8	3TTY-E	<i>Bacillus circulans</i> sp. <i>alkalophilus</i>	Mesophile	39.9	1.9	29
9	4OIF-B	<i>Geobacillus</i> <i>stearothermophilus</i>	Thermophile	39.1	2.0	29
10	4UOZ-C	<i>Bifidobacterium animalis</i> <i>subsp. lactis</i> Bl-04	Mesophile	38.6	2.2	29

84

85

86

87

88

89

90

91

92

93

94

95

96

97

98

99

100

101 **Table S5. Trends for halo-, psychro-, and thermoadaptation compared to mesophilic proteins**
 102

	hla_bga	Halophilic¹	Psychrophile²	Thermophilic³	
Sequence analysis	pI	decreased	decreased	Decreased	slightly decreased
	Grand average hydrophobicity	increased	increased	Increased	increased
	Aliphatic amino acids (%)	decreased	slightly increased	slightly decreased	increased
	Positively charged amino acids, R, K and H (%)	slightly increased	slightly increased	Decreased	increased
	Negatively charged amino acids, D and E (%)	increased	increased	Decreased	increased
	Small amino acids, G and A (%)	increased	increased	Decreased	decreased
	Hydrophobic residues, F, I, L, V, M (%)	decreased	slightly decreased	Increased	increased
	Polar residues (%)	decreased	decreased	Increased	decreased
	Non-polar residues (%)	decreased	decreased	Decreased	slightly increased
	Aspartic acids (%)	decreased	decreased	Decreased	increased
	Glutamic acids (%)	increased	increased	slightly increased	increased
	Aromatic residues (%)	increased	decreased	slightly increased	increased
	Proline amino acids (%)	increased	decreased	Decreased	decreased
	Arginine amino acids (%)	increased	increased	slightly increased	increased
	Structural analysis	Positive residues among total number of surface residues (%)	decreased	decreased	slightly increased
Negative residues among total number of surface residues (%)		increased	increased	Increased	increased
Polar residues among total number of surface residues (%)		decreased	decreased	Increased	decreased
Non-polar residues among total number of surface residues (%)		decreased	decreased	Decreased	decreased
Aromatic residues among total number of surface residues (%)		decreased	decreased	slightly increased	increased
Amino acids that form helices (%)		decreased	increased	increased	increased
Amino acids that form strands (%)		decreased	decreased	decreased	increased
Amino acids with bulky hydrophobic side chains (F, I, L) in the protein surface (%)		decreased	decreased	increased	increased
Hydrogen bonds (intra and inter)		increased	decreased	increased	decreased
Salt bridges		increased	decreased	decreased	decreased

103 The thermophilic, psychrophilic, halophilic and mesophilic enzymes of varying length were used for the
 104 analysis which was reflected in the lower hydrogen bonds and salt bridges compared to hla_bga
 105 [13][14][15].
 106
 107
 108

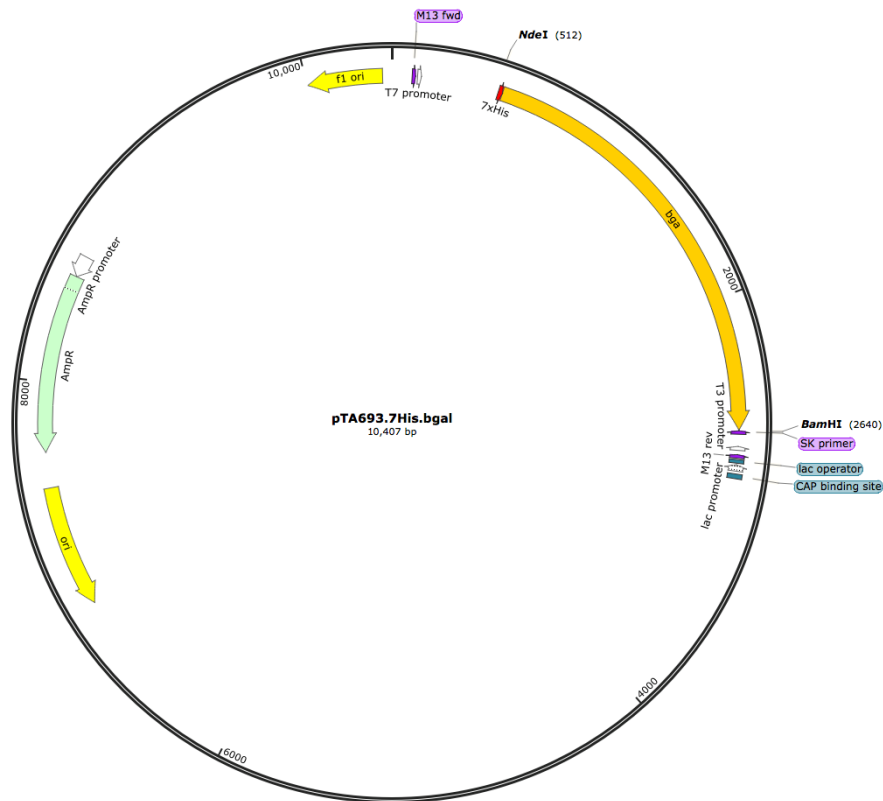
109 **Table S6.** Differences in residue RMSF values (Δ RMSF) between 47 and 10 °C for eight functionally
110 relevant residues.
111

Δ RMSF (Å) between 47 and 10 °C			
Residue ^a	Hla_bga	Mesophile (3TTS)	Thermophile (1KWG)
R102	0.216	0.232	0.127
N140	0.052	0.121	0.053
E141	0.074	0.091	0.037
Y266	0.059	0.276	0.047
E312	0.036	0.196	0.074
W320	0.261	0.556^b	0.436
E360	0.396	0.367	0.187
H363	0.222	0.484	0.221
average	0.164	0.290	0.148

112 ^a Numbering from hla_bga, ^b Values above the threshold for significance (0.5 Å) indicated by Dong *et al.*
113 2018 for a similar temperature rise (15 to 42 °C) are in bold.

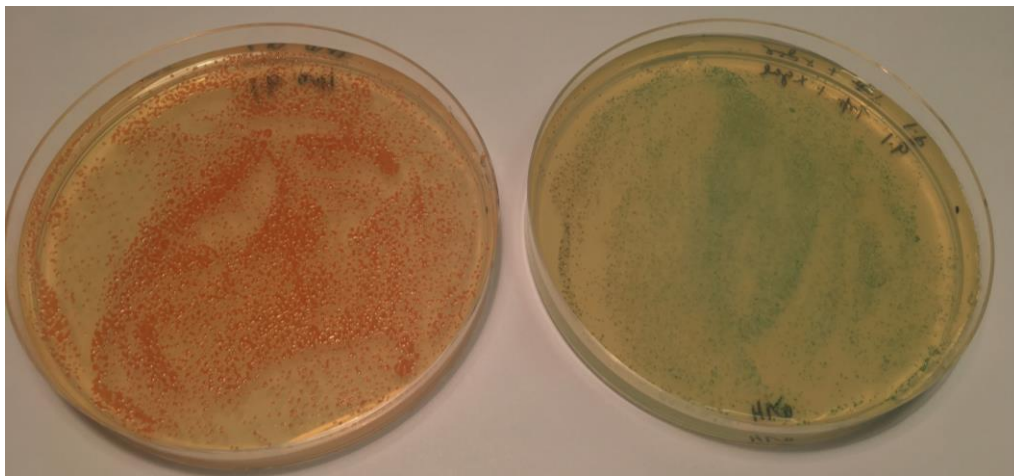
114

115



116
 117 **Figure S1.** Shuttle vector for the expression of *bga* in *Haloferax volcanii*. The *NdeI* and *BamHI*
 118 restriction sites were used to introduce the *bga* gene.

119



Control

β -galactosidase transformants

120

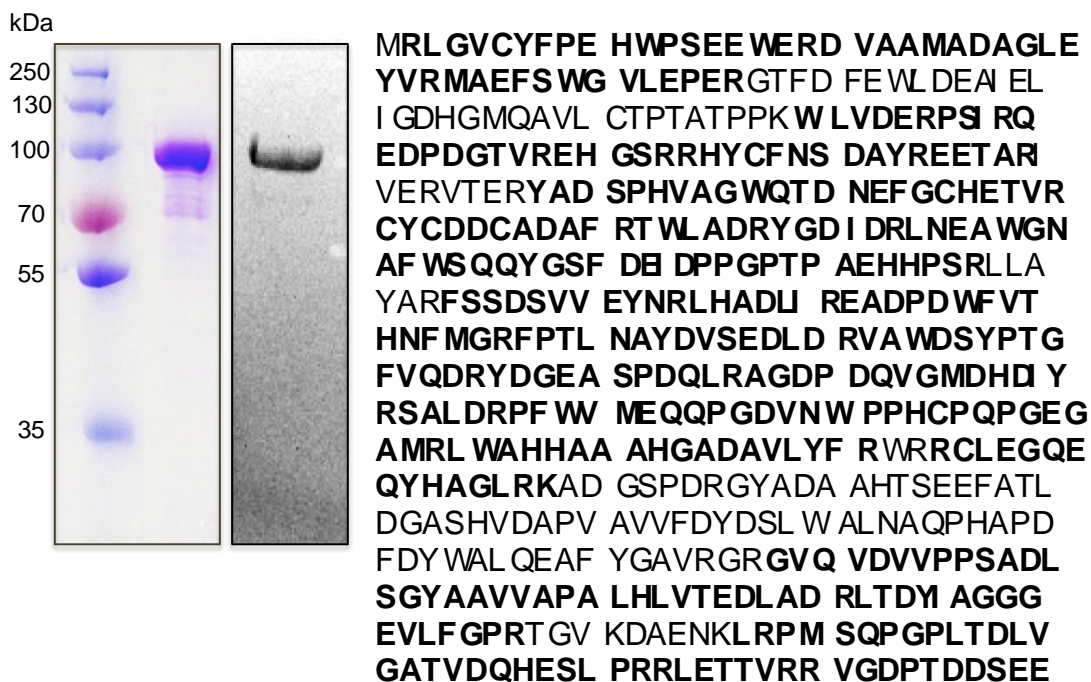
121

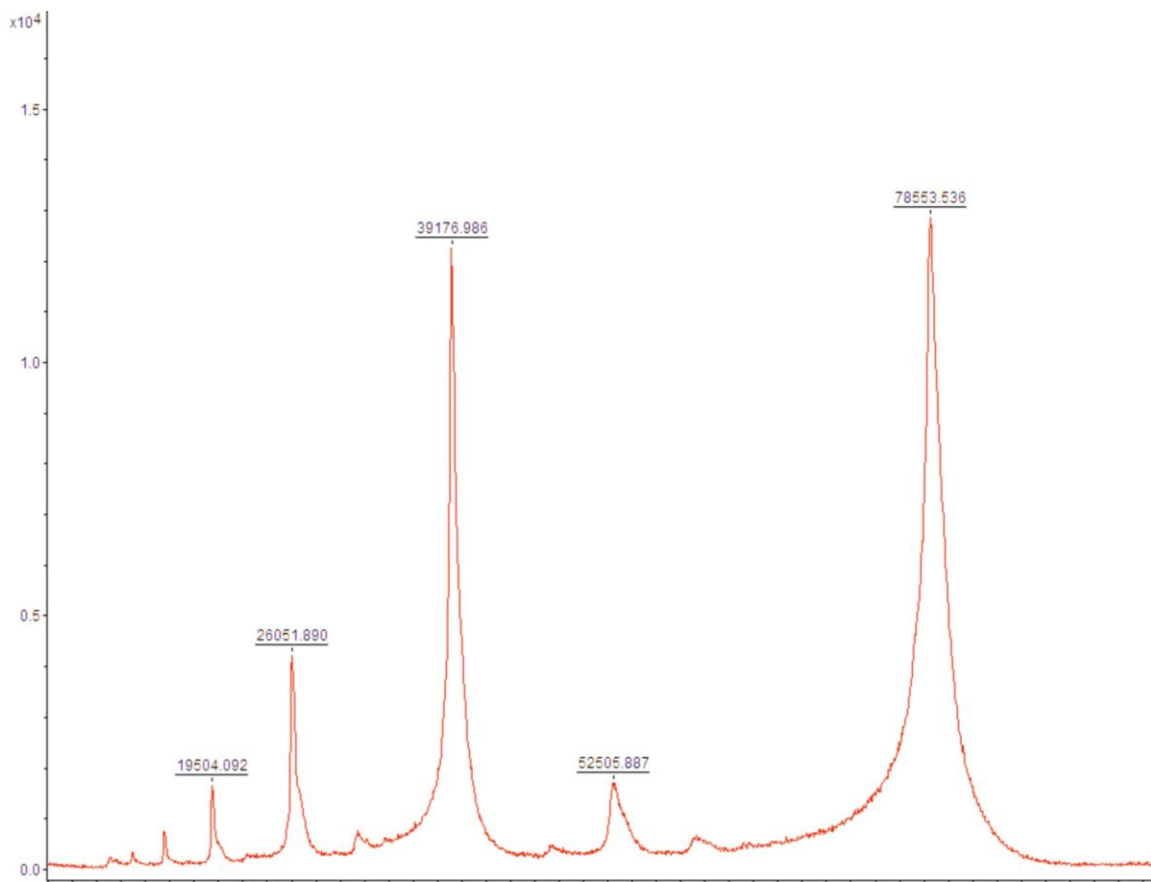
122 **Figure S2.** X-gal hydrolysis. When the β -galactosidase gene is in a gene fusion with the pTA693 vector
 123 in *Haloferax volcanii*, X-gal is hydrolyzed indicating the *bga* protein is produced.

124

125 A

B





134

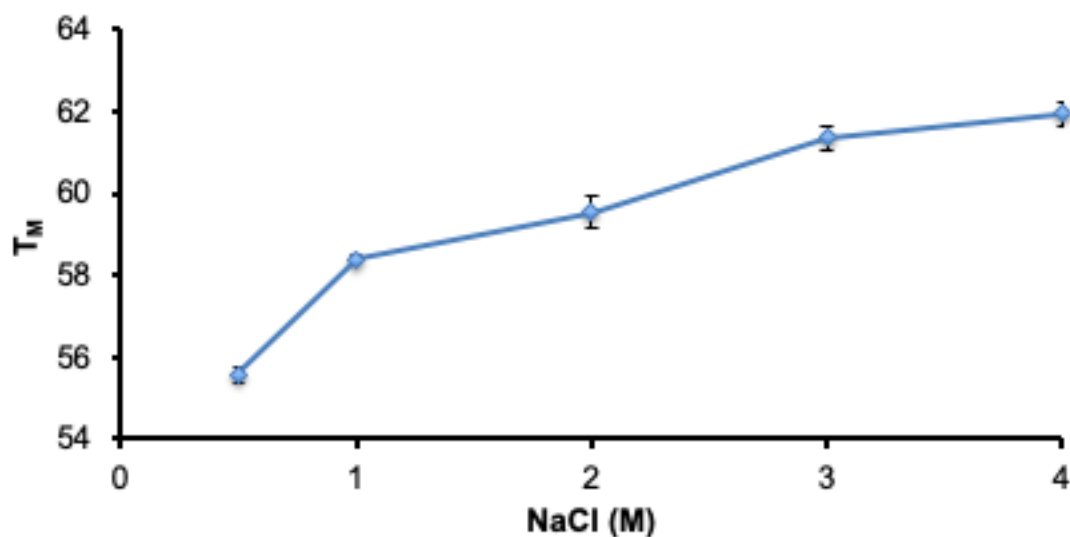
135

136 **Figure S4.** MALDI-TOF analysis of purified β -galactosidase: β -galactosidase shows two major peaks
137 around 78.55 kDa (calculated size: 79147 including 7His) and 39.176 kDa (dimer).

138

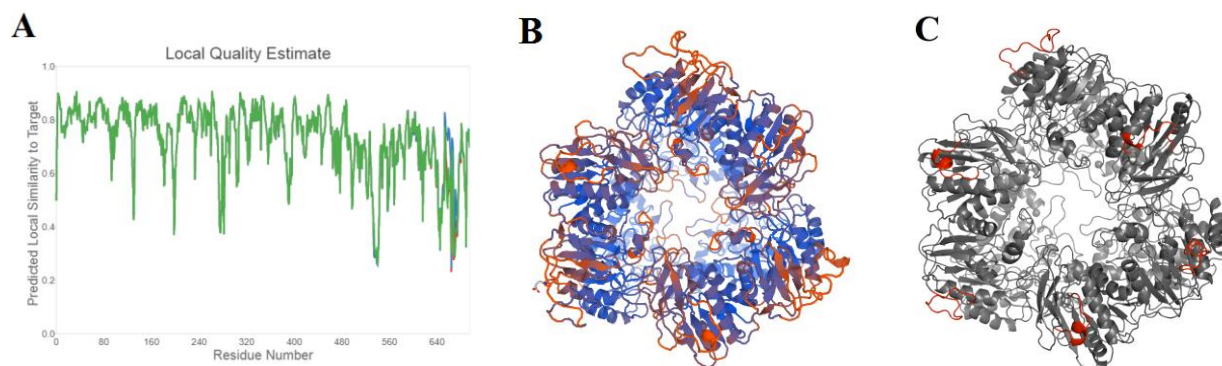
139

140



141
142
143
144
145

Figure S5. Measured melting temperatures at different salt concentrations



146
147

Figure S6. Structural assessment of the hla_bga homology model produced by SwissModeller [16]. (A) Local quality estimates are shown for each amino acid position of the monomer chain A. The overall global score of the homology model is 0.73 ± 0.05 , global score ranges between 0 to 1 method used was QMEANDisco [16]. (B) Local quality scores shown on the structure model, red color indicates poor score and blue color indicates good score. Pictures were derived from the server. (C) Modelled hla_bga, the modelled loop regions not visible in the electron density are shown in magenta color.

154
155
156
157
158
159
160

161 T-Coffee

162
163 Hla_bga MR LGVCYFPEHWPSE--EWERDVAAMADAGLEYVRMAEFSWGVLEPERGT
164 1KWG M-LGVCYYPEHWPKE--RWKEDARRMREAGLSHVRIGEFAWALLEPEPGR
165 4UZS LWYGGDYNPDQWPE--EVWDDDIRLMKKAGVNLVSVGIFSWAKIEPEEGK
166 3TTS IWYGGDYNPEQWDK--ATMEEDMRMFNLAGIDVATVNVFVSWAKIQRDEVS
167 4UNI IWFGADYNPDQWPE--DVQDEDIRLMKQAGVNIIVSLAIFSWANIETSDGN
168 5XB7 ILFGAAYYDEYIIPRDLDRIDTDMEMMTRAGINIVIRIGESTWSTCEPQPGH
169 4OIF ILHGGDYNPDQWLDPRDILQADLELMKLSHTNTFTVGVFAWSALEPEEGV
170 5E9A LLHGADYNPEQWLDHPDVLVRDVEMMKEARCNVMSVGVFVSWALEPEEGR
171 6Y2K MKLGVCYYPEHWPKE--RWVEDAQHMRRIGIQYVRVGEFVSWSTIEPTPGE
172 : * * : * : . : :* . :

173
174 Hla_bga FDFEWLDEAIELIGDHGMQAVLCTPTATPPKWLVDPERPSIRQEDPDGTVR
175 1KWG LEWGWLDEAIATLAAEGLKVVLTPTATPPKWLVDRIPEILPVDREGRRR
176 4UZS YDFDWLDRADIKLGKAGIAVDLASATASPPMWLTAHPEVLWKDERGDTV
177 3TTS YDFTWLDDIIERLTKENIYLCLATSTGAHPAWMAKKYPDVLVDYEGRKR
178 4UNI FEFDWLDRVIDKLYKAGIAVDLASATASPPMWLTAHPEVLRDEQGHVI
179 5XB7 FDWTHIDRALDAATNAGINIVIGTPTYAVPTWLVAMYPDVLATTPAGEP-
180 4OIF YRFEWLDKVFDDIYRIGGRVILATPSGARPAWLSQKYPEVLRVNAARVRQ
181 5E9A YTFDWMQVLRNLHENGISVFLATPSGARPAWMSQKYPQVLRVGRDRVPA
182 6Y2K LHWEWLDESLEDILHSQGLKVILGTPTATPPKWLVDHRPSMLAKDEAGRVR
183 : :* : . : : : * * : * . :

184
185 Hla_bga EHGSRRHYCFNSDAYREETARIVERVTERYADSPHVAGWQTDNEFGCHET
186 1KWG RFGGRRHYCFSSPVYREEARRIVTLLAERYGGLEAVAGFQTDNEYGCHDT
187 4UZS WPGAREHWRPTSPVFREYALNLCRRMAEHYKGNPYVVAWHVSNIEYGCHNR
188 3TTS KFGGRHNSCPNSPTYRKYAKILAGKLAERYKDHPQIVMWHVSNIEYGGY--
189 4UNI WPGARQHWRPTSPFTRYALRLCREMAEHYKDNPAIVSWHVGNEYGCHNY
190 5XB7 HYGARQIMNIVNPAYRLYGERVIRSLISHVAQQPCVIGYQVDNETKYYS
191 4OIF LHGGRHNHCFTSSVYREKTQHINRLLAERYGDHPALLMWHVSNIEYGGE--
192 5E9A LHGGRHNHCMSPPVYREKQMLMNGQLAKRYAHPAVIGWHISNEYGGE--
193 6Y2K GFGSRRHYTFASLEYREECRRMVTMMAERYGHHPAVASWQTDNEYGCHDT
194 * . * . : * : : : : : * * : * . *

195
196 Hla_bga VRCYCDDCADAFRTWLADRY-G-DIDRLNEAWGNFWSQQYGSFDEIDPP
197 1KWG VRCYCPRCQEA FRGWLEARY-G-TIEALNEAWGTAFWSQRYRSFAEVELP
198 4UZS -FDYSDDAMRAFQKWKCKRY-K-TIDAVNEAWGTAFWAQHMFSEIIPP
199 3TTS --CYCDNCEKQFRVWLKERY-G-TLEALNKAWNTSFWSHTFYDWDEIVAP
200 4UNI -FDYSDDAVQAFREWCRRDY-G-TIDKVNAAWGTFWFSQRLNSFEEIIPP
201 5XB7 V---SHDMQVMFIKQLRHEFKN-DLEALNEAYGLDYWSNRINAWEDF--P
202 4OIF --CHCNLCQEA FREWLKCKY-NHDLDALNAAWWTFWFSHTYTDWSQIESP
203 5E9A --CHCDTCQGFQFRDWLKARY-V-TLDALNKAWWTFWFSHTYTDWSQLESF
204 6Y2K VLSYAEADLAAFRLWLAEKY-G-TVEALNKAWGNVFWFSMDYRSFDEIELP
205 . * . : : : * * : * : : : . *

206
207 Hla_bga GPTPAEH-----HPSRLLAYARFSSDSVVEYNRLHADLIREADP-DWV
208 1KWG HLTVAEP-----NPSHLLDYRFASDQVRAFNRLOVEILRAHAP-GKFL
209 4UZS RYIGD-GN--F-MNPKLLDYKRFSSDALKELYIAERDVLESITP-GLPL
210 3TTS NALSEEWSGNRTNFQGISLDYRRFQSDSLLLECFCMERDELKRWTP-DIPV
211 4UNI RYVGGEGN--F-TNPGRLDFKHFCS DALKEFFCAERDVLSEVTP-NIPL
212 5XB7 DLTGS-I-----NESLRARDFRDRQVAEYLAWQASIIREYMRDDQFI
213 4OIF SPIGEHT-----IHGLNLDWKRFTDQTISSFFENEIVPLRELTP-HIPI
214 5E9A SPQGENG-----VHGLNLDWRRFNTDQVTRFCSEEIRPLKAENP-ALPA
215 6Y2K NLTVTEA-----NPSHRLDFQRCCSDQVVAFNKLQVDILREHSA-GRDL
216 . : : * . :

```

217
218 Hla_bga THNFM-----GR-----FPTLNAYDVSEDLDRVAWDSYPTGFVQDR
219 1KWG THNFM-----GF-----FTDLDAFALAQDLDFASWDSYPLGFTDLM
220 4UZS TTNFM-----VSA-----GGSMLDYDDWGAEVDFVSNHDHYFTPGEA--
221 3TTS TTNLM-----GF-----YPELDYFKWAKEMDVVSWDNYPMSMDTP--
222 4UNI TTNFM-----VSA-----SQNTLDYDDWAHEVDFVSNHDHYFTPGSW--
223 5XB7 THNFDYEWGRHSYGL-----QPAVDHFRAARALDICGVDIYHPSEDA--
224 4OIF TTNFM-----ADTHDLIPFQGLDYSKFAKHLDVDI SWDAYPAWHNDWE
225 5E9A TTNFM-----EY-----FNDYDYWKLAGVLD F I SWDSYPMWHTRQD
226 6Y2K VHNYM-----GF-----FTAFDHHKVGQDL DVASWDSYPLGSLDKE
227 . * . : * . * *
228
229 Hla_bga -Y-DGEASPDQLRAGDPDQVGMHDHIYRSALDR-PFWVMEQQ-PGDVNWIP
230 1KWG PL-PPEEKLR YARTGHPDVA AFHHDLYRGVGRG-RFWVMEQQ-PGPVNWA
231 4UZS -----HFDEVAYAASLMDG I SRKEPWFQMEHS-TSAVNWR
232 3TTS -----FSFTAMAHNLMRGLKSGQPFMLMEQT-PGVQNWQ
233 4UNI -----HIDELAYSASLVDG I SRKKPWFLMEQS-TSAVNWR
234 5XB7 -----LTGKEIAFGGDMARSAGGG-NYLVLETQAQQQHGWL
235 4OIF ST-----ADLAMKVGFINDLYRSLKQQ-PFLLMECT-PSLVNWH
236 5E9A DI-----GLAAYTAMYHDLMRTLKQKPFVLMEST-PSFTNWQ
237 6Y2K PLYTEDEKHTYLRVGHDPDAGAFHHDLYRGCNG-RLWIMEQQ-PGPVNWA
238 . . : * . . *
239
240 Hla_bga PHCPQPGEGAMRLWAHHAAGADAVLYFRWRRCLEGQEQYHAGLRKADG
241 1KWG PHNPS PAPGMVRLWTWEALAHGAEVVSYFRWRQAPFAQE QMHAGLHRPDS
242 4UZS PINYRAEPGSVVRDSLAVAMGADAICYFQWRQSKAGAEKWHSSMVPHAG
243 3TTS PYNSAKRPGVMRLWSYQAVAHGADTVMFFQLRRSVGACEKYHGAVIEHVG
244 4UNI EINPRKEPGE LIRDSMLHLAMGADAICYFQWRQSRSGAEK FHSAMLPLAG
245 5XB7 P-----YPGQLRLQAYSHLASGADGIMYWHWHHSIHNSFETYWRGLLSHDF
246 4OIF KVNKAKRPGMHFLSSMQMIAHGSDSILYFQWRKSRGSEKFKHGAVVDHDN
247 5E9A PTSKLLKPGMHILSSLQAVAHGADSVQYFQWRKSRGSEKFKHGAVVDHVG
248 6Y2K PHNPTPADGAVRLWTWEAFSHGAELVSYFRWRQAPFGQE QMHAGLLRPDA
249 * : : * : : : : . * . :
250
251 Hla_bga S-PDRGYADAHTSEEFATLD-----GASHVDAPVAVVFDYDSLW
252 1KWG A-PDQGF FEAKRVAEELAALA-----LPPVAQAPVALVFDYEA AW
253 4UZS E-DSQIFRDVCELGADLGRLSDE-----GLMGTKTVKSKVAVVFDYESQW
254 3TTS HEHTRV FRECAELGKELQQLGDT-----ILD-ARSEAKVAVMYDWENRW
255 4UNI E-HSQIYRDVCALGADLDTLSDA-----GILRSKLSKARVAIVQDIQSEW
256 5XB7 E-SNPTYEEAGRFGREIGDPR-----IGDTLSHLSKRNAVAILASNESLT
257 4OIF RTDSRVFQEVAEVKGALKKMSGI-----VG-TNRPAEVAILYDWENNW
258 5E9A HIDTRV GREVAELGSILSALAPV-----AG-SRVEAKVAIIFDWESRW
259 6Y2K Q-EAEAAKEATLVAQEVKVLAE SIGLDADELMSLPSAGKVALMFDYDACW
260 : . . ** : : . :
261
262 Hla_bga ALN----A--QPHAPDFDYWALQEAFYGAVRGRGVQVDVPPSAD---LS
263 1KWG IYE----V--QPQGAEWSYLGLVYLFYSALRRLGLDVDVPPGAS---LR
264 4UZS ATE----YTANPTQ-QVDHWTEPLDWFALADNGITADVVPVRS D---WD
265 3TTS ALE----LSSGPSI-ALNYVNEVHKYYDALYKQNIQTDMI SVEED---LS
266 4UNI ATE----HTATPTQ-HIREWTEPLDWF AAFANRGVTADVTPIHAQ---WD
267 5XB7 ALSWFHIETGFPMGGTLTYNDVLR SIYDALFELNVEVDFLPADASADQLA
268 4OIF ALN----DAQGFAAETKRYPQTLVQHYRPFWERDI PVDVITKEHD---FS
269 5E9A AMD----DAMGPRNAGLHYENTVADHYRALWAQGI AVDVINADCD---LQ
270 6Y2K SLD----I--QPQS RAYRYFFWCYRMYEAMRELGLSVDIVPSNAP---LD
271 . : . . : * .
272

```

273
274
275 Hla_bga GYAAVVAPALHLVTEDLADRLTDYIAGGGEVLFGRPTGVKDAENKLRPMS
276 1KWG GYAFAVVPSLPIVREEALEAFREA---EGPVLFGPRSGSKTETFQIPKEL
277 4UZS SYEIAVLPCVYLLSEETSRRVREFVANGGKLFVTTYTGLSDENDHIWLGG
278 3TTS KYKVVIIAPVMYMKPGFAERVERFVAQGGTFVTTFFSGIVNENDLVTLGG
279 4UNI TYDAVVI PCVYLFSEEMAERLRTFVRNGGKAFVTTYSSALADEHDLRHTEG
280 5XB7 GYSLVIAPALYTTDQQTIDRLARYVKNGGHLATMRSFVADENVKVVHDK
281 4OIF RYKLLIAPMLYL VSEETIARLKEFVANGGTLVMTYISGIVDEHDLAYLGG
282 5E9A GYDLVIAPMLYMRVREGVGERISAFVQAGGRFVATYWSGIVNETDLCFLNG
283 6Y2K MYELLVLPQAHAHITPELQNLNSY---QGVLLAGPRTGSKTETYQIPENL
284 * : * . * . :
285
286 Hla_bga QPGPLTDLVGATVDQHESE-L---PRRLE--TTVRRVGDPTDDSEEIAAPP
287 1KWG PPGPLQALLPLKVVVRVES-L---PPGLL--EVAEGA-----LGR
288 4UZS YPGSIRDVVGVRVEEFAP-MGNMMPGAL--DHLDL-----NG
289 3TTS YPGELRNVMGIWAEIIDA-L---LPGHQ--NEIVLRQ----DWGGLR-GS
290 4UNI WPGLIGDVVGVRIEEHCP-LGTLFPGML--DHLDVS-----NG
291 5XB7 APHHLVDIFGMTYNQFTRPM---GVSLKCPDTLADL-----AGA
292 4OIF WHQDLREMFGMEPIETDT-L---YPRDR--NSVHYRG-----RS
293 5E9A FPGPLRPVLGIWAEIDS-L---TDEQH--NSVAGVE---GNALGLS-GP
294 6Y2K APGPLASLLPLTVERVDA-L---PEHTQ--PAVSGR-----WGA
295 : :. . :
296
297 Hla_bga VSFRTWAEWLD--PDAEPQYAYDVGDP--ADGRPAVVNTVGDGQVTYC
298 1KWG FPLGLWREWVE--APLKPL-LTF-----QDGKGA----LYREGRYLYL
299 4UZS TVAHDFADVITSTADTSTVLASYKAERWTGMNEVPAIVANGYGDGRTVYV
300 3TTS YSCGILCDVIH--AETAEVLAEY GADYY---KGTPVLTRNKFGNGQSYV
301 4UNI TVVHDLADVIDAIADDTTVLATFEADPATGMDGRAAITVHPYHEGGVAYI
302 5XB7 -SANDFIEMLSP-APETHVLAWYDHYA---WDSYAAITRHAFSGSDAQWV
303 4OIF YELKDYATVIK--IHAATVEGVYEDDFY---ADTPAVTSNQYKKGQAYYI
304 5E9A YRASQLCEVIH--LEGAALATYGDFFY---AGNPAVTVNLYGKGQAYYV
305 6Y2K GKLKHWHEQIK--TELPCL-LKD-----DGGNPV----LMGEGRHYL
306 : : . * :
307
308 Hla_bga GVWPESDLADALASDLLDRAGVRYAERL--PDGVRIGY--R---GGRTWV
309 1KWG AAWPSPELAGRLLSALAAEAGLKVL-SL--PEGLRLRR--R---GTWVFA
310 4UZS GCRLGRQGLAKSLPAMLGSMGLS DLAG--DGRVLRVERADAAAASHFEFV
311 3TTS ASSPDADFLQGLIANLCEEQGVKPLL--NTPDGVEVAER-VKNGTSYLFV
312 4UNI AGKLRDGI SQSLPEICAALGFELDADPRAGDVLRVVREQ-EDGAI FEFL
313 5XB7 GTQLQADAWRTVLAEALS NAGVHTP-GMELAGTVCVRS GTNTAGDVTYTL
314 4OIF GGRLEDQFHRDFYQELMEKLDLRPVL FVKHEKGVSVQAR-QAPECDYVFI
315 5E9A ASRNDQQFHADFF TALAKEMKLPRAINTPLPEGVTAARR-TDGESEFI FL
316 6Y2K GSCIDNTLLKASLAKLSEVAGLSTY-YL--PKGVRVRE--R---GNVIFA
317 . . : :
318
319 Hla_bga TNFTSDRLRLPEIDPESLAVDDTDRDGFDPMADD-DK--DSSAD-----
320 1KWG FNYGPEAVEAPA-----SE-GA--RFLLG-----
321 4UZS FNRTHEPVTVDV-----EG-EA-IAASLAH-----
322 3TTS MNHNAEEMTFDA-----GASRQR-DLLTGK-----
323 4UNI FNRRTRNTVTADR-----PA-GDMLICSLAT-----
324 5XB7 LNYSGSPITFRA-----PA-SG--TFLLGHPTDDG
325 4OIF MNFTEEKQAVVL-----EE-KVK-DLFTGE-----
326 5E9A QNYNADNQTVAL-----PQ-DYQ-DIVHGG-----
327 6Y2K FNYSSNTVVFEP-----Q-NA--ELVIG-----
328 * .

```

329
330
331
332 Hla_bga      -----GIVVGPYGVAVIEGDCVD
333 1KWG        -----SRRVGPYDLAVW--E---
334 4UZS        -----VDDGRATIDPTGVVVLRL----R
335 3TTS        -----TISGQATIPARGVMILER---A
336 4UNI        -----DSTDKVTLEPNGVLAF-----R
337 5XB7        EQAVTAETPVTVGDAVTLPRWGVDIIVGRQPT
338 4OIF        -----EIVGEIMLDKYEVRVVEKR--R
339 5E9A        -----NLPRKLTLPAFGCQILTR---K
340 6Y2K        -----SMCLGAADVVAIWKKQ---
341
342

```

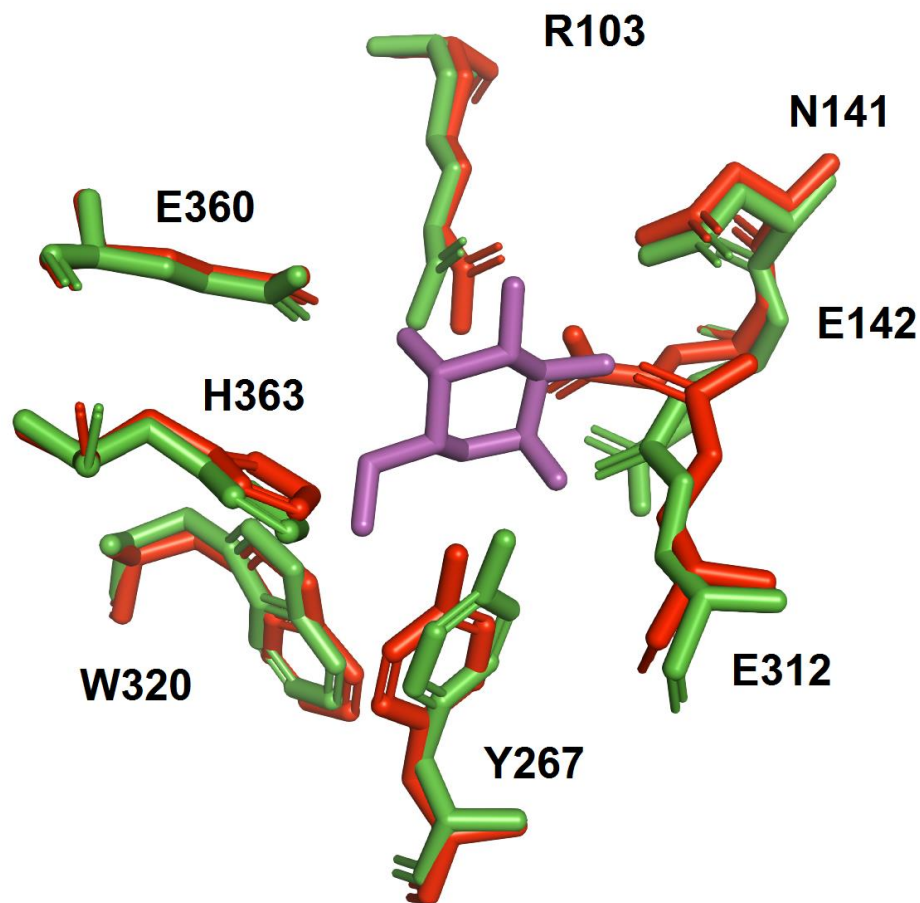
343 **Figure S7.** Sequence alignment obtained with T-Coffee [17]. The red blocks represent the β -galactose
344 binding site, predicted flexible loops of hla_bga (532-543 and 657-672) are highlighted in yellow shade.
345 *Halorubrum lacusprofundi*, hla; *Thermus thermophilus* A4, 1KWG; *Bifidobacterium bifidum* S17, 4UZS;
346 *Bacillus circulans* sp. Alkalophilus, 3TTS; *Bifidobacterium animalis* subsp. lactis BI-04, 4UNI;
347 *Bifidobacterium* species 5XB7; *Geobacillus stearothermophilus*, 4OIF; *Rahnella* sp. R3, 5E9A;
348 *Marinomonas* ef1, 6Y2K

349

350

351

352

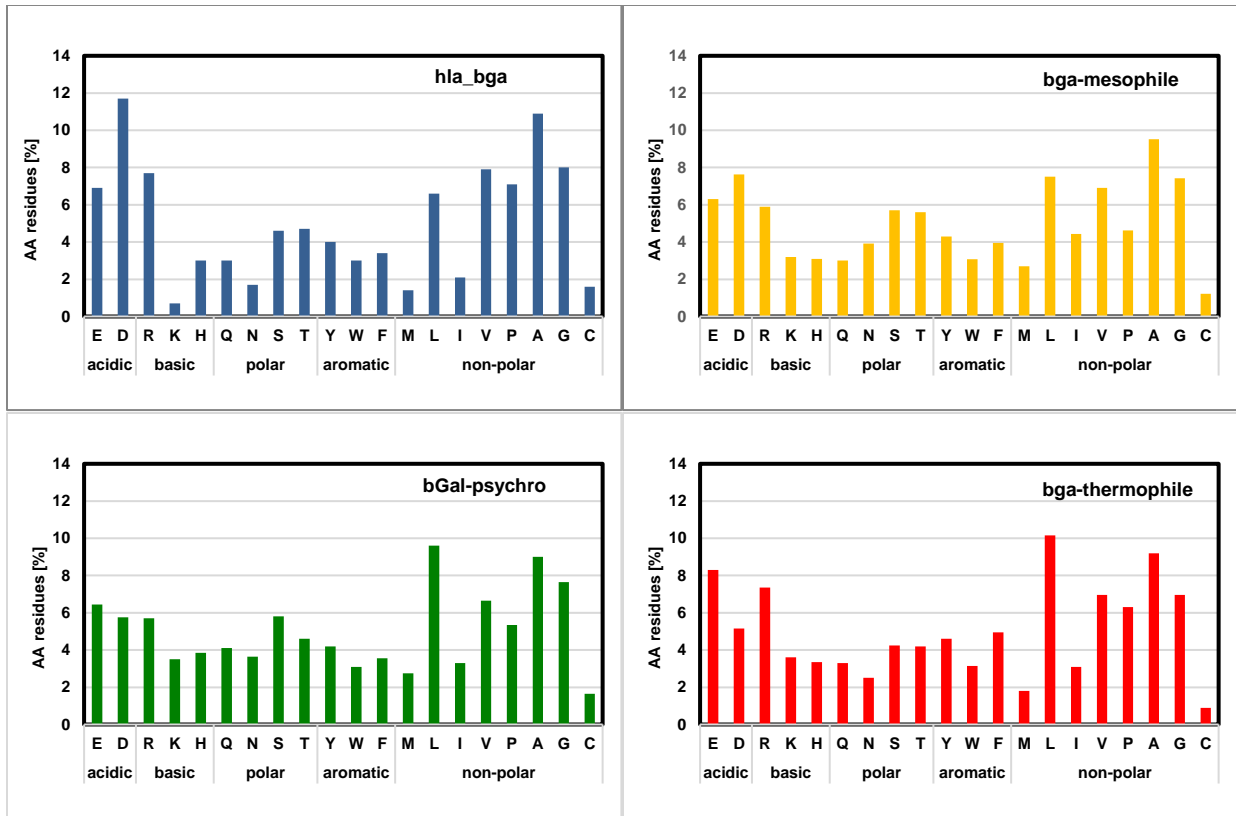


353

354

355 **Figure S8. β -D-galactose binding pocket.** The binding pocket of hla_bga based on conserved catalytic
356 motif of various β -Gal structures. The amino acids residues of hla_bga, β -Gal-tA4 (1KWK) and β -D-
357 galactose are red, green and magenta respectively. 1KWK and 1KWG are β -Gal-tA4 with β -D-galactose
358 ligand and without β -D-galactose ligand, respectively.

359

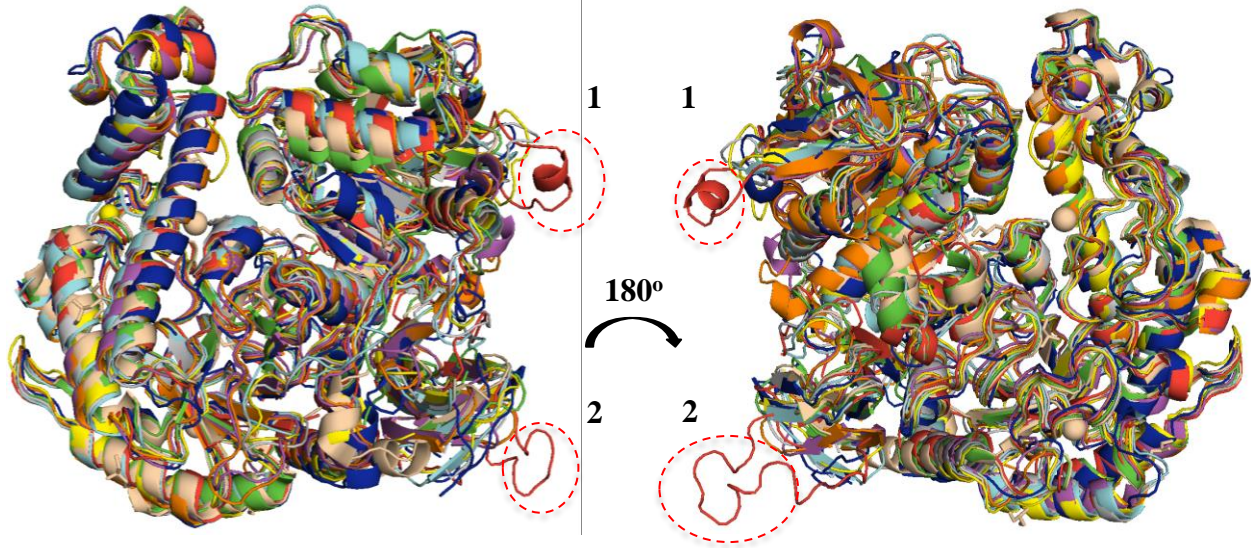


360

361 **Figure S9.** Ratio of amino acids in hla_bga and its structural homologs. *Halorubrum lacusprofundi*,
362 hla_bga; bga-mesophile (3TTS, 4UZS, 4UNI, 5XB7); bga-psychrophile (5E9A, 6Y2K); bga-thermophile
363 (1KWG, 4OIF).

364

365



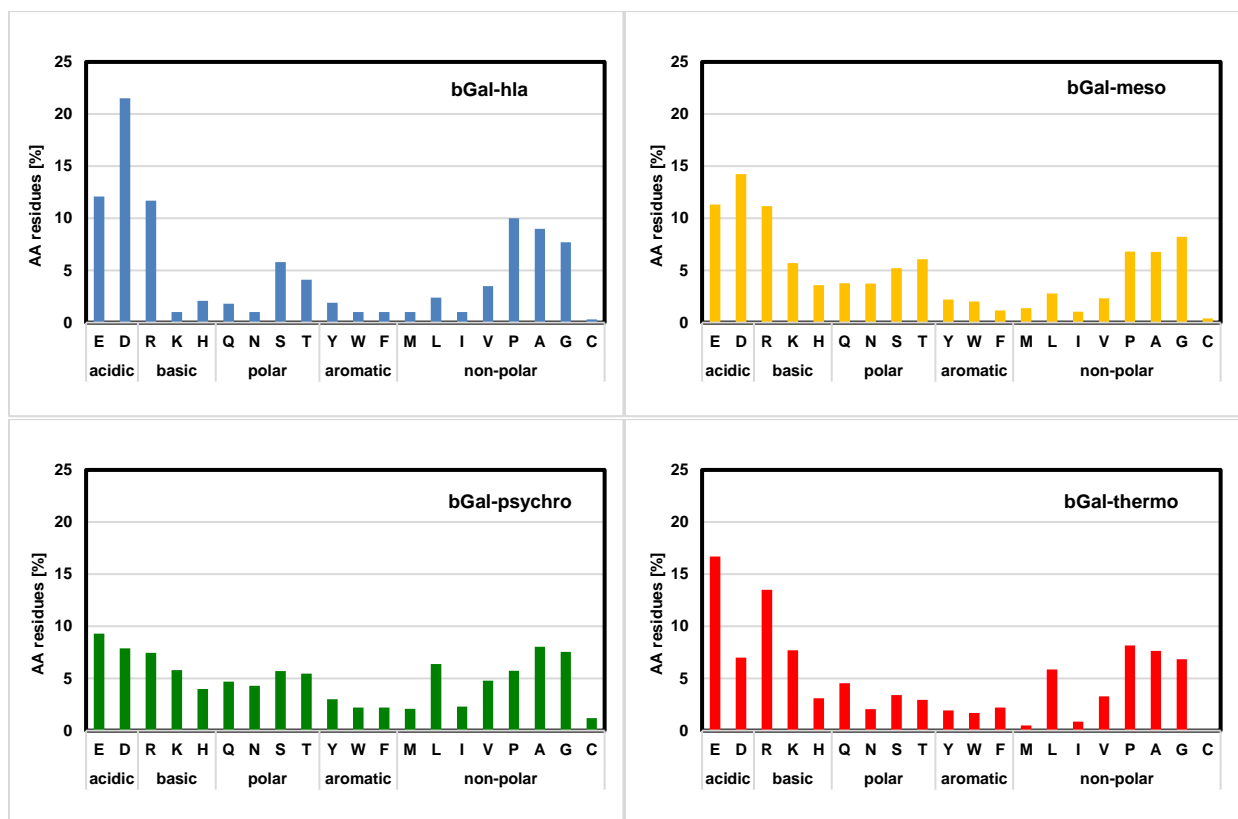
366

367

368 **Figure S10. Superimposed β -Galactosidase monomers:** 1 and 2 represent the flexible loop regions 532-
369 543 and 657-672, respectively, of the modeled bga_hla. *Halorubrum lacusprofundi*, hla (red); *Thermus*
370 *thermophilus* A4, 1KWG (green); *Bacillus circulans* sp. *Alkalophilus*, 3TTS (yellow); *Bifidobacterium*
371 *animalis* subsp. lactis BI-04, 4UNI (orange); *Bifidobacterium bifidum* S17, 4UZS (pink); *Marinomonas*
372 ef1, 6Y2K (wheat); *Rahnella* sp. R3, 5E9A (grey); *Geobacillus stearothermophilus*, 4OIF (cyan);
373 *Bifidobacterium* species 5XB7 (blue).

374

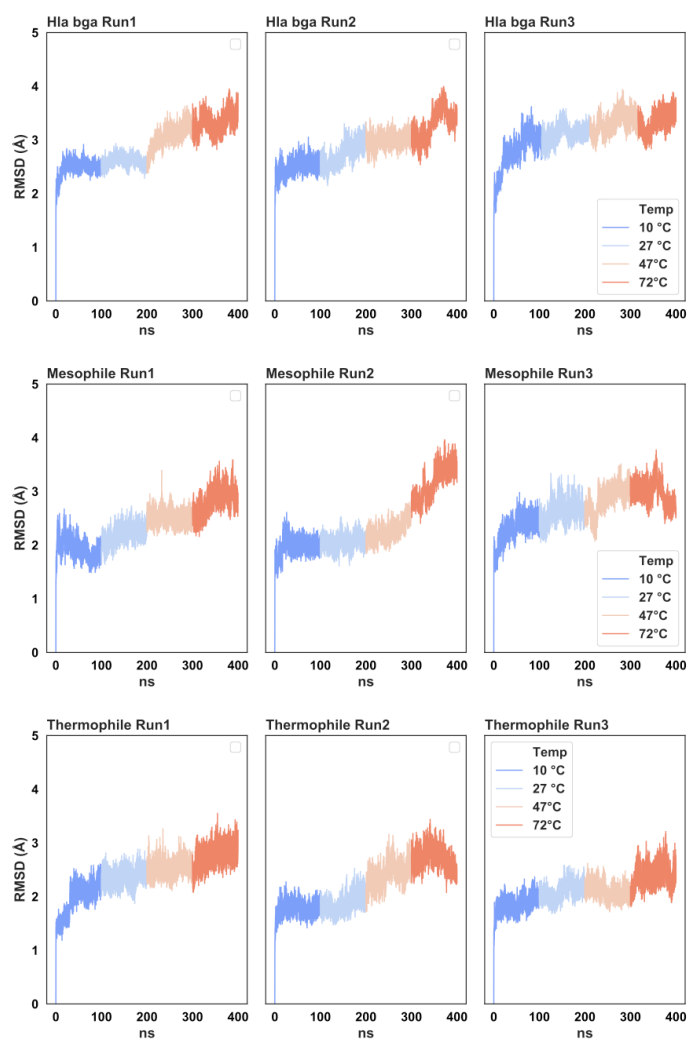
375
376



377

378
379
380
381
382
383
384
385

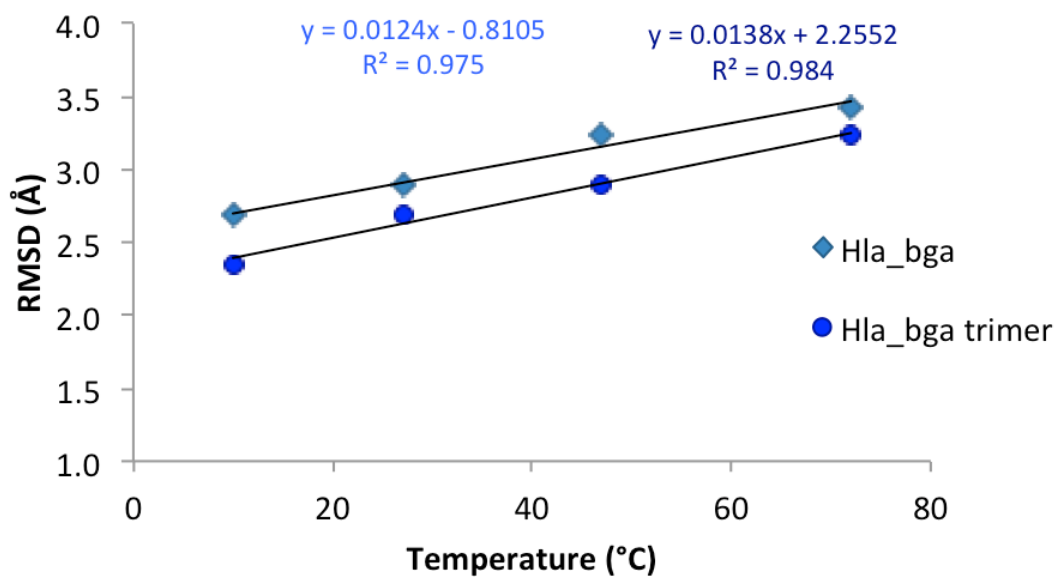
Figure S11. Ratio of amino acids on the solvent-exposed surface in hla_bga and its structural homologs. *Halorubrum lacusprofundi*, hla_bga; bga-mesophile (3TTS, 4UZS, 4UNI, 5XB7); bga-psychrophile (5E9A, 6Y2K); bga-thermophile (1KWG, 4OIF).



386

387 **Figure S12.** Backbone RMSD plots over time for the three independent simulations of the three
 388 investigated systems at the four explored temperatures (10, 27, 47 and 72 °C).

389

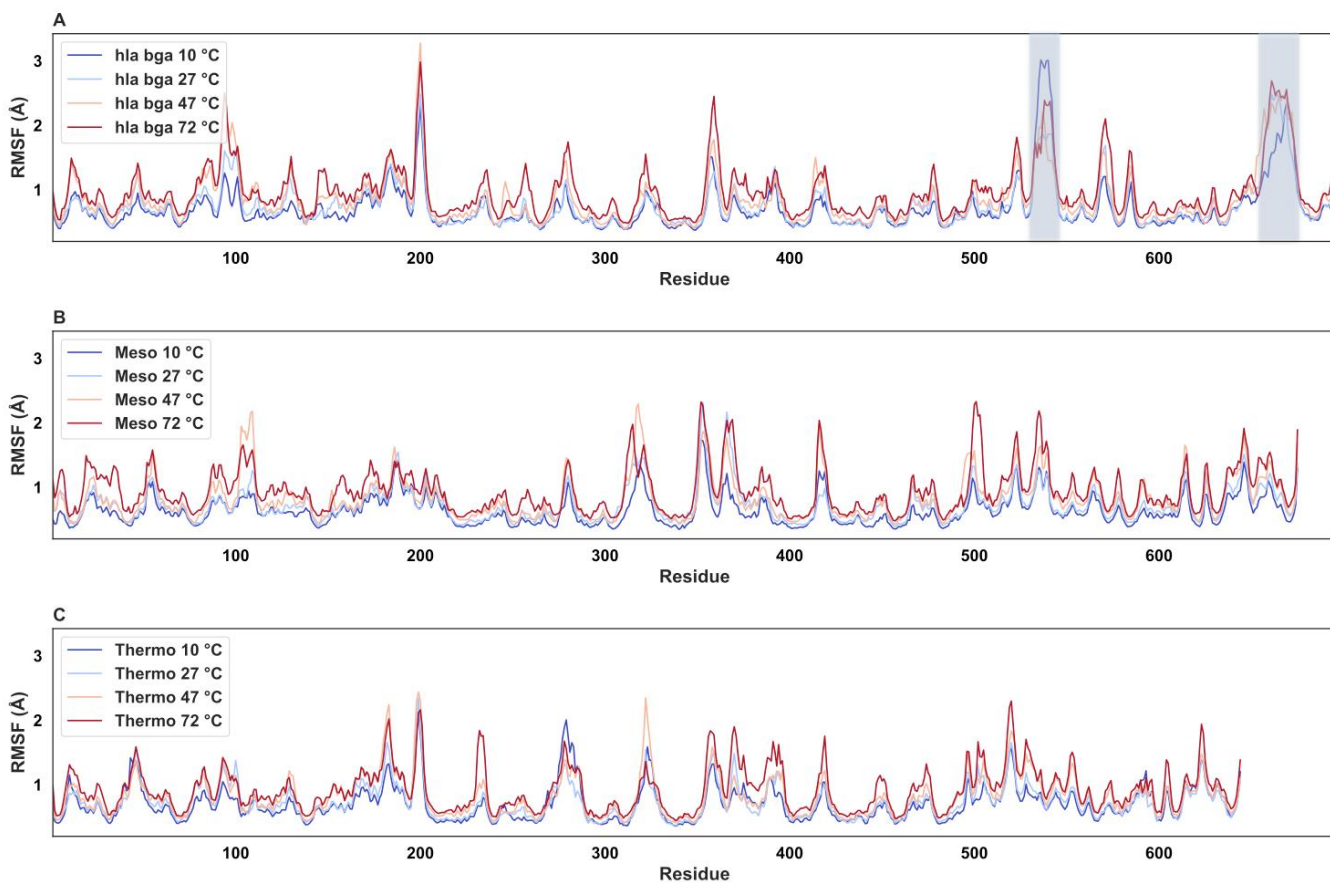


390

391 **Figure S13.** Effect of temperature on the hla_bga monomer and trimer backbone RMSD. Values are
 392 averaged on the last 20 ns of the simulations for each system. Corresponding trendlines are shown with
 393 relative correlation coefficients (R2) and equations.

394

395



396

397 **Figure S14.** RMSF values averaged over the last 20 ns of the three simulations ran for each investigated
 398 system at 10, 27, 47 and 72 °C. Hla_bga loops 532-543 and 657-672 are highlighted by a blueish shadow.

399

400
401
402
403
404
405
406
407
408
409
410
411
412
413
414
415
416
417
418
419
420
421
422
423
424
425
426
427
428
429
430
431
432
433
434
435
436
437
438
439
440
441
442
443

References

1. DasSarma, S.; Capes, M.D.; Karan, R.; DasSarma, P. Amino acid substitutions in cold-adapted proteins from *Halorubrum lacusprofundi*, an extremely halophilic microbe from Antarctica. *PLoS One* **2013**, *8*, e58587.
2. Hidaka, M.; Fushinobu, S.; Ohtsu, N.; Motoshima, H.; Matsuzawa, H.; Shoun, H.; Wakagi, T. Trimeric crystal structure of the glycoside hydrolase family 42 β -galactosidase from *Thermus thermophilus* A4 and the structure of its complex with galactose. *Journal of molecular biology* **2002**, *322*, 79-91.
3. Ohtsu, N.; Motoshima, H.; Goto, K.; Tsukasaki, F.; MATsUzAWA, H. Thermostable β -galactosidase from an extreme thermophile, *Thermus* sp. A4: enzyme purification and characterization, and gene cloning and sequencing. *Bioscience, biotechnology, and biochemistry* **1998**, *62*, 1539-1545.
4. Fan, Y.; Yi, J.; Hua, X.; Feng, Y.; Yang, R.; Zhang, Y. Structure analysis of a glycosides hydrolase family 42 cold-adapted β -galactosidase from *Rahnella* sp. R3. *RSC advances* **2016**, *6*, 37362-37369.
5. Fan, Y.; Hua, X.; Zhang, Y.; Feng, Y.; Shen, Q.; Dong, J.; Zhao, W.; Zhang, W.; Jin, Z.; Yang, R. Cloning, expression and structural stability of a cold-adapted β -galactosidase from *Rahnella* sp. R3. *Protein expression and purification* **2015**, *115*, 158-164.
6. Godoy, A.S.; Camilo, C.M.; Kadowaki, M.A.; Muniz, H.d.S.; Espirito Santo, M.; Murakami, M.T.; Nascimento, A.S.; Polikarpov, I. Crystal structure of β 1 \rightarrow 6 - galactosidase from *Bifidobacterium bifidum* S17: trimeric architecture, molecular determinants of the enzymatic activity and its inhibition by α - galactose. *The FEBS journal* **2016**, *283*, 4097-4112.
7. Maksimainen, M.; Paavilainen, S.; Hakulinen, N.; Rouvinen, J. Structural analysis, enzymatic characterization, and catalytic mechanisms of β - galactosidase from *Bacillus circulans* sp. alkalophilus. *The FEBS journal* **2012**, *279*, 1788-1798.
8. Solomon, H.V.; Tabachnikov, O.; Lansky, S.; Salama, R.; Feinberg, H.; Shoham, Y.; Shoham, G. Structure–function relationships in Gan42B, an intracellular GH42 β -galactosidase from *Geobacillus stearothermophilus*. *Acta Crystallographica Section D: Biological Crystallography* **2015**, *71*, 2433-2448.
9. Tabachnikov, O.; Shoham, Y. Functional characterization of the galactan utilization system of *Geobacillus stearothermophilus*. *The FEBS journal* **2013**, *280*, 950-964.
10. Viborg, A.H.; Fredslund, F.; Katayama, T.; Nielsen, S.K.; Svensson, B.; Kitaoka, M.; Lo Leggio, L.; Abou Hachem, M. A β 1 - 6/ β 1 - 3 galactosidase from *Bifidobacterium animalis* subsp. *lactis* B 1 - 04 gives insight into sub - specificities of β - galactoside catabolism within *Bifidobacterium*. *Molecular microbiology* **2014**, *94*, 1024-1040.
11. Viborg, A.H.; Katayama, T.; Arakawa, T.; Hachem, M.A.; Leggio, L.L.; Kitaoka, M.; Svensson, B.; Fushinobu, S. Discovery of α -L-arabinopyranosidases from human gut microbiome expands the diversity within glycoside hydrolase family 42. *Journal of Biological Chemistry* **2017**, *292*, 21092-21101.
12. Mangiagalli, M.; Lapi, M.; Maione, S.; Orlando, M.; Brocca, S.; Pesce, A.; Barbiroli, A.; Camilloni, C.; Pucciarelli, S.; Lotti, M., et al. The co-existence of cold activity and

- 444 thermal stability in an Antarctic GH42 β -galactosidase relies on its hexameric quaternary
445 arrangement. *The FEBS Journal* *n/a*, doi:10.1111/febs.15354.
- 446 13. Graziano, G.; Merlino, A. Molecular bases of protein halotolerance. *Biochim Biophys*
447 *Acta* **2014**, *1844*, 850-858, doi:10.1016/j.bbapap.2014.02.018.
- 448 14. Santiago, M.; Ramírez-Sarmiento, C.A.; Zamora, R.A.; Parra, L.P.J.F.i.m. Discovery,
449 molecular mechanisms, and industrial applications of cold-active enzymes. **2016**, *7*,
450 1408.
- 451 15. Karshikoff, A.; Ladenstein, R.J.P.e. Proteins from thermophilic and mesophilic
452 organisms essentially do not differ in packing. **1998**, *11*, 867-872.
- 453 16. Waterhouse, A.; Bertoni, M.; Bienert, S.; Studer, G.; Tauriello, G.; Gumienny, R.; Heer,
454 F.T.; de Beer, T.A P.; Rempfer, C.; Bordoli, L., et al. SWISS-MODEL: homology
455 modelling of protein structures and complexes. *Nucleic Acids Research* **2018**, *46*, W296-
456 W303, doi:10.1093/nar/gky427.
- 457 17. Zimmermann, L.; Stephens, A.; Nam, S.Z.; Rau, D.; Kübler, J.; Lozajic, M.; Gabler, F.;
458 Söding, J.; Lupas, A.N.; Alva, V. A Completely Reimplemented MPI Bioinformatics
459 Toolkit with a New HHpred Server at its Core. *J Mol Biol* **2018**, *430*, 2237-2243,
460 doi:10.1016/j.jmb.2017.12.007.

461